

Trajectory of the stellar flyby that shaped the outer Solar System

Received: 8 December 2022

Accepted: 29 July 2024

Published online: 04 September 2024

 Check for updatesSusanne Pfalzner¹✉, Amith Govind¹ & Simon Portegies Zwart²

Unlike the Solar System planets, thousands of smaller bodies beyond Neptune orbit the Sun on eccentric ($e > 0.1$ and $i > 3^\circ$) orbits. While migration of the giant planets during the early stages of Solar System evolution could have induced substantial scattering of trans-Neptunian objects (TNOs), this process cannot account for the small number of distant TNOs ($r_p > 60$ au) outside the planets' reach. The alternative scenario of the close flyby of another star can instead produce all these TNO features simultaneously, but the possible parameter space for such an encounter is vast. Here we compare observed TNO properties with thousands of flyby simulations to determine the specific properties of a flyby that reproduces all the different dynamical TNO populations, their locations and their relative abundances, and find that a $0.8^{+0.1}_{-0.1} M_\odot$ star passing at a distance of $r_p = 110 \pm 10$ au, inclined by $i = 70^{+5}_{-10}$, gives a near-perfect match. This flyby also replicates the retrograde TNO population, which has proved difficult to explain. Such a flyby is reasonably frequent; at least 140 million solar-type stars in the Milky Way are likely to have experienced a similar one. In light of these results, we predict that the upcoming Vera Rubin telescope will reveal that distant and retrograde TNOs are relatively common.

The Solar System planets accumulated from a disk of dust and gas that once orbited the Sun. Therefore, the planets move close to their common plane on near-circular orbits. About 3,000 small objects have been observed to orbit the Sun beyond Neptune ($r_p > 35$ au); surprisingly, most move on eccentric and inclined orbits^{1,2}. Therefore, some force must have lifted these trans-Neptunian objects (TNOs) from the disk where they formed and altered their orbits markedly. One popular hypothesis is that the planets originally were in a more compact configuration; the TNOs formed between them and were scattered outwards when the planets moved to their current locations (see, for example, refs. 1,3–8).

However, three distinct TNO dynamical groups are incredibly challenging to explain from the original planet scattering: (i) the cold Kuiper belt objects moving on nearly circular orbits close to the plane, (ii) the Sedna-like TNOs orbiting at large distances ($r_p > 60$ au) on highly eccentric orbits ($e > 0.5$) and (iii) TNOs with high inclination ($i > 60^\circ$)^{9–13}. While only three Sedna-like objects and few highly inclined TNOs are

known so far, they are the make-or-break test for any outer Solar System formation theory. Their existence, especially the observed clustering among the Sedna-like and high-inclination TNOs, is unlikely to stem from scattering by the planets^{1,14}.

Here, we build on a completely different hypothesis for the TNOs' origin^{15–17}. In this model, the TNOs formed in the outer Solar System (>30 au) and the close passage of another star catapulted them to their current orbits. This hypothesis was initially overlooked as such close flybys were deemed too rare. However, recent Atacama Large Millimeter Array observations reveal that close stellar flybys seem to be relatively common^{18–23}. Recently, this scenario has gained renewed interest due to simulations showing that flybys could produce a cold Kuiper belt population and Sedna-like objects^{14,24,25}. These proof-of-principle studies considerably strengthened the flyby hypothesis. However, the possible flyby parameter space has remained relatively large, and the resulting predictions vague. More precise predictions are essential to decide between the competing hypotheses. Here, we present the

¹Jülich Supercomputing Centre, Forschungszentrum Jülich, Jülich, Germany. ²Leiden Observatory, Leiden University, Leiden, The Netherlands.

✉e-mail: s.pfalzner@fz-juelich.de

Table 1 | Flyby scenarios reproducing the known TNO population

	Emphasis on	$M_p [M_\odot]$	r_p [au]	i [°]	ω [°]	R_d [au]
A	Sedna-like	0.8	110	70	80	150–300
B	Cold Kuiper belt	0.8	110	70	90	150
C	ETNOs	0.8	110	65	60	150

The first column gives the scenario identifier, column 2 the TNO subgroup emphasized when determining the best fit, column 3 M_p , column 4 r_p , column 5 i , column 6 ω and column 7 the assumed pre-flyby disk size. ETNOs, extreme TNOs.

essential next step—we provide the close-to-exact parameters of the potential outer Solar System shaping flyby. The resulting predictions are distinct and testable using the ~40,000 TNOs awaiting discovery when the Vera C. Rubin Observatory becomes operational²⁶. The TNOs orbiting in the opposite direction to the planets ($i > 90^\circ$)—so-called retrograde TNOs—may be the key to this analysis.

Results

Our exhaustive numerical parameter study consists of over 3,000 individual simulations modelling the effect of a stellar flyby on a planetesimal disk surrounding the Sun extending to 150 au and 300 au, respectively. Such sizes have been observed to be typical for protoplanetary and debris disks^{27,28}. We vary the mass of the perturber, M_p , its perihelion distance, r_p , and the relative orientation of its path in terms of inclination, i , and angle of periastron, ω , and the size of the disk, R_d .

We systematically rejected any flyby that failed to quantitatively match the observed TNO population. This means that any successful candidates had to reproduce the location in the a (semi-major axis), e , i parameter space and the relative population sizes of the cold Kuiper belt objects and the Sedna-like objects. The latter are particularly important as, unlike the resonant TNOs, their relative numbers and orbits are largely unaffected by interactions with Neptune after the flyby, expressed by the Tisserand parameter $T_N < 3.05$. In addition, we demanded that the planet orbits remain unperturbed (for details, see Methods). Only three flybys met our strict criteria for an excellent quantitative match to the observed TNOs (Table 1). These three flybys produced the hot, cold and Sedna-like TNOs in the observed relative quantities and in the right places in the multidimensional parameter space. Each best-fit model emphasized different TNO dynamical groups in the selection process. Still, their parameters are so similar that one can combine them into a single flyby scenario with a remarkably small error bar.

For a parabolic flyby, we find that a star with mass $M_p = 0.8^{+0.1}_{-0.1} M_\odot$ at $r_p = 110 \pm 10$ au inclined by $i = 70^\circ \pm 5^\circ_{-10^\circ}$ and an angle of periastron of 60° – 90° provides the best candidate for an outer Solar System shaping flyby on the basis of current data. The spatial orientation is given relative to the plane of the pre-flyby disk. For an illustration of the flyby dynamics, see Fig. 1 and Supplementary Video 1. The past flyby orbital parameters are shown by Fig. 2 (left). We performed higher-resolution simulations for models A–C with 10^5 tracer particles and modelled two disk sizes (150 au and 300 au—models A1 and A2, respectively). Interestingly, these parameters are fairly consistent with those of another flyby scenario²⁹, which argues that a $1.8 M_\odot$ star would have passed the Solar system at $r_p = 227$ au inclined by 17° – 34° . The different mass can be explained by the type of encounter studied: where ref. 29 adopted an exchange interaction to abduct Sedna from the intruder, here we argue that Sedna (and the other Kuiper belt objects) are native to the Solar System.

The flyby probably happened several billion years ago, so how much would the orbital parameters change on such a timescale? Investigating the long-term evolution of the TNO population is computationally expensive. Therefore, we studied only the period of 1 Gyr after the flyby. The general outcome remains very similar (Fig. 2 (middle)).

The changes include an increase in low-inclination TNOs, improving the match to the cold TNO population and filling in the low-inclination distant TNOs missing immediately after the flyby. Thus, the long-term evolution leads to an even better fit.

The final model delivered a surprise: the best-fit flyby created retrograde TNOs despite them not being part of the selection process. So far two retrograde TNOs have been confirmed—2008 KV₄₂ and 2011 KT₁₉, both having relatively small periastron distances ($r_p < 30$ au, $a > 30$ au) and inclined by 103.41° and 110.15° , respectively. An additional TNO is suspected of moving on a retrograde orbit—2019 EE₆—but its orbit is currently not well constrained. It is more distant ($r_p > 30$ au) and may be closer to the plane ($>150^\circ$).

Eventually, high-inclination TNOs could be crucial when deciding between different hypotheses. Retrograde TNOs themselves provide a challenge for the planet instability model. Adding a distant planet (Planet Nine) appeared to solve the problem^{30,31}. This combined model can account for retrograde TNOs with $r_p < 30$ au and $i < 150^\circ$ such as 2008 KV₄₂ and 2011 KT₁₉ (Fig. 1 in ref. 30). However, distant, highly inclined TNOs ($r_p > 30$ au, $i > 150^\circ$), if they exist, may provide a challenge also for the Planet Nine model.

Conversely, retrograde TNOs might also be the key to determining the primordial size of the solar system disk. The maximum inclination of retrograde TNOs is directly related to the primordial disk size (Fig. 3). The inclinations of 2008 KV₄₂ and 2011 KT₁₉ (103.41° and 110.15°) demand that the Sun's primordial debris disk must have extended to at least $R_d \geq 65$ au. Close to the plane retrograde TNOs would argue for an even larger size ($R_d \geq 150$ au). Using this relation, retrograde TNOs detected in the future will enable stringent bounds to be set on the primordial disk size.

Currently, only the nearest and brightest TNOs are observable, and high-inclination and very eccentric objects are challenging to detect. The right-hand panels of Fig. 2 supply a sneak preview of the TNO discoveries we expect from the flyby scenario presented here. They show that the clustering among the known highly inclined TNOs¹³ and Sedna-like objects is part of a much larger pattern caused by the flyby. It will be interesting to see this pattern emerge when more TNOs are discovered. Although the pattern becomes slightly less distinctive on Gyr timescales due to secular effects (see middle panels), the clustering itself persists (Fig. 2 (middle)).

The information about the flyby parameters enables us to predict how the relative sizes of different TNO dynamical groups will change when the observable space expands (Supplementary Fig. 1 and Supplementary Table 1). Matching the observations, Sedna-like TNOs make up only about 0.1% of all TNOs in models A–C in the current observationally accessible space. However, this will increase to 7% by the end of the ten-year observation campaign of the Vera Rubin telescope as more distant TNOs become observable. Likewise, we anticipate an increase in the fraction of retrograde TNOs from 0.15% to about 5% as the discovery space expands. Although some of the expected retrograde TNOs may orbit close to the plane, we foresee most of them moving at high inclinations from the plane.

However, we caution against overinterpreting Fig. 2. To some extent, we expect the non-detection of TNOs in covered areas. Neither the size nor the structure of the primordial solar disk is known. Any change—smaller size or ring structures—in the primordial disk leads to ‘holes’ in the parameter space indicated in Fig. 2. Indeed, such gaps could even help to determine the solar disk's structure before the flyby. Conversely, if TNOs are found in areas not predicted by Fig. 2 even after including the long-term evolution, this would challenge the presented hypothesis. However, its falsifiability makes the flyby hypothesis methodologically very strong.

So far, we have concentrated on the bound TNO population beyond 30 au. However, while leaving the planetary orbits undisturbed, the flyby injects many TNOs (~9% of the initial disk mass m_i) into the area inside 30 au. These injected TNOs move with high eccentricity

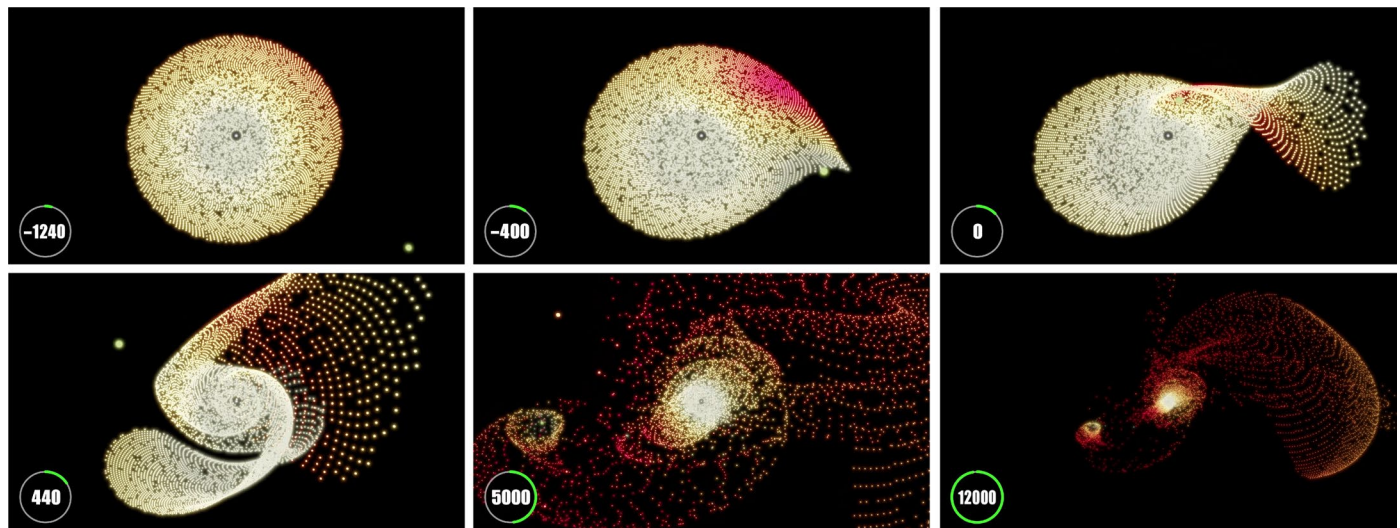


Fig. 1 | Simulation snapshots of model A1. The perturber star approaches from the bottom right. The sequence shows the typical appearance of two spiral arms, the loss of matter that becomes unbound and the capture of some material by the perturber star. The time is given in years relative to the time of

periastron passage. For the first four snapshots, the size of the real area is kept constant; the last two plots show a zoom-out. The colours indicate the velocities of the test particles relative to the Sun. The complete dynamics is illustrated in Supplementary Video 1.

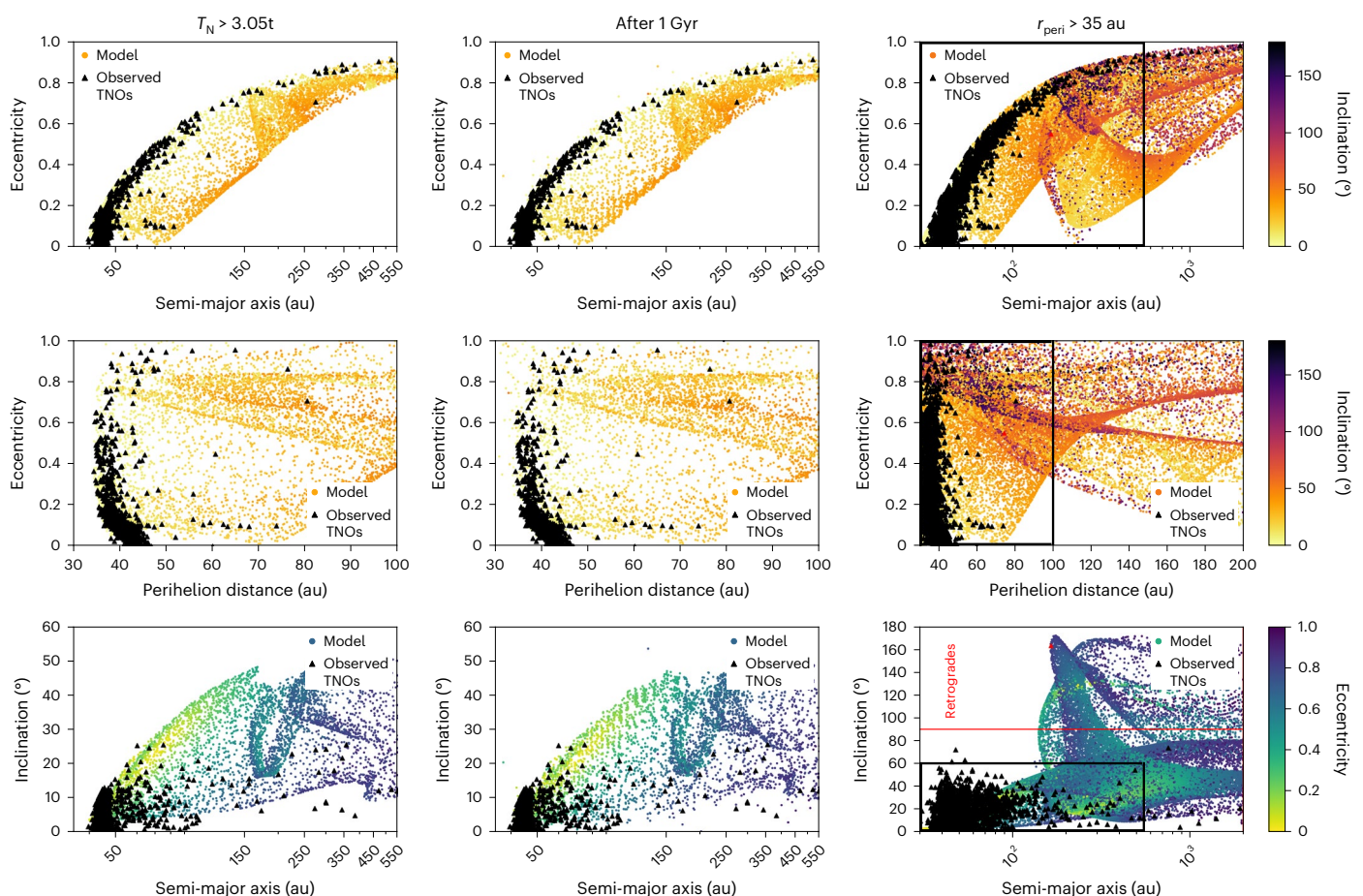


Fig. 2 | Comparison of TNO orbital parameters between observations and simulation (model A2). The coloured symbols show the simulation result, and the black triangles depict the observed TNOs. Left and middle panels: situation 12,000 yr and 1 Gyr after the periastron passage. Here, only the subset of the resulting population with $35 \text{ au} < r_p < 100 \text{ au}$, $a < 2,000 \text{ au}$, $i < 60^\circ$ is shown, roughly corresponding to the current observationally accessible area. Only objects with $T_N > 3.05$ were chosen for the comparison. Right panel: zoom-out

that includes all particles. For comparison, the black box indicates the area shown in the left and middle panels. The right panel can be used to predict the properties of the expected TNO discoveries. There the red triangle indicate the nominal positions of the recently discovered retrograde TNOs. The red line shows the divide between pro- and retrograde TNOs. See Supplementary Figs. 4–6 for equivalent plots for models A with disk size 150 au, B and C.

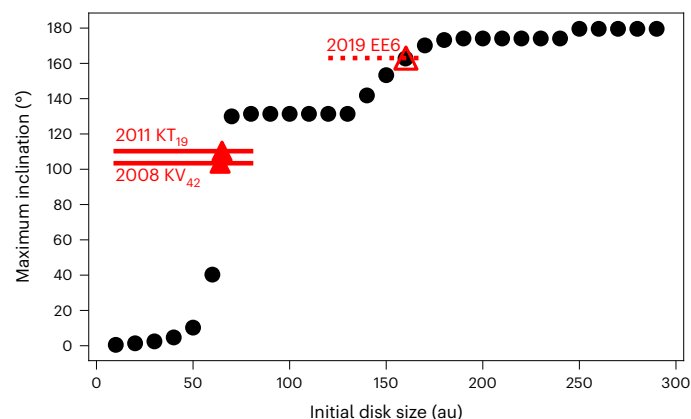


Fig. 3 | Disk size versus inclination correlation. Dependence of the maximum inclination on primordial disk size. The filled red triangles show the properties of the confirmed retrograde TNOs, the open red triangle indicates the inclination of the yet to be confirmed retrograde TNO 2019 EE6.

($e > 0.4$) and high inclination ($> 30^\circ$), regularly revisiting the trans-Neptunian region (60–200 au). At the same time, a considerable fraction (26%) of the TNOs become unbound from the Sun (Supplementary Fig. 2), and the perturber captures 8.3% of the material initially bound to the Sun (model A1). While moving on highly eccentric orbits, some of these captured solar TNOs come incredibly close to the perturber star ($r_p^{\min} = 0.73$ au). These TNOs move well within the ice lines of this system, where volatiles evaporate.

Discussion

The known TNO population is subject to many different biases (for a discussion see refs. 32,33), and probably represents only a fraction ($< 1\%$ – 10%) of the entire population. New TNOs are constantly being discovered, some with entirely unexpected orbital properties^{13,34}. Thus, searching for flyby parameters best fitting the observations presented here can only be a first step. Once a significant portion of the TNOs is known, this procedure must be repeated, and the flyby parameters adjusted accordingly. Despite these reservations, we expect the final best-fit parameters to be similar. After all, the model must still account for the Kuiper belt, Sedna-like and retrograde TNOs at the currently known positions in the multidimensional parameter space. Alternative hybrid schemes combining planet scattering with one or more flybys have been suggested³⁵. However, it is an open question whether such hybrid scenarios have predictive power.

When would this flyby have occurred? Close encounters are most frequent during the first 10 Myr of a star's life when it is still part of its birth cluster. Simulations find that typically 8%–15% of all solar-type stars experience an encounter reducing the unperturbed area to 30–50 au in favourable environments (similar to NGC 2244 and M44)³⁶. Even in low-density clusters, $\sim 1\%$ of solar-type stars experience such an encounter. Putting this number in perspective, in the first 10 Myr of their lives, at least 140 million solar-type stars in the Milky Way (possibly ten times more) have experienced an encounter similar to the Sun's. In $\sim 10\%$ of these cases, the encounter was with a similar-mass perturber $M_p = 0.6$ – $1.0 M_\odot$ at approximately the same periastron distance ($r_p = 90$ – 130 au) as the Sun's flyby. Close flybys become less frequent after the solar birth cluster expands and dissolves at the end of the star formation process. However, the 4.55 Gyr that has passed since the Solar System formed can more than outbalance the much lower encounter frequency, summing to a probability of 20%–30% likelihood for a late encounter²⁴. However, due to the stellar velocity dispersion increasing with the Sun's age, these flybys would be mainly on highly hyperbolic orbits. Hyperbolic flybys are much less efficient in exciting the orbits of TNOs. Therefore,

the question of whether a later flyby could lead to a similarly good match requires further study.

The flyby scenario does not exclude either the planets forming in a more compact configuration or the existence of a primordial Oort cloud. Planet migration could have scattered additional objects into the trans-Neptunian region, contributing to the hot Kuiper belt population without altering the Sedna-like or retrograde TNO populations. Even if the planets were located at their current positions at the time of the flyby, they would all have been unaffected by the flyby except Neptune. If Neptune were at its current distance at the time of the flyby, it would have been shielded from the effect of the flyby in 25% of cases, staying in the gravitational shadow of the perturber—meaning flying behind the perturber star (Supplementary Fig. 2).

If the Oort cloud existed before the flyby, it would have been severely affected, but not erased. A flyby of the given parameters would have left a sufficiently large number of TNOs ($\sim 15\%$) bound to the Sun to account for the current estimates of the Oort cloud mass. Moreover, the Oort cloud might have been simultaneously enriched by TNOs with $a \gg 10^4$ au originally belonging to the outer disk ($80 \text{ au} < r_p < R_d$) and planetesimals initially part of the potentially existing perturber Oort cloud³⁷.

Finally, we may speculate on whether the probability of the perturber's planetary system developing life was increased by the flyby. The probability would have been higher if the flyby happened not during the first 10 Myr but later when pre-forms of life had already developed.

Conclusion

We have demonstrated that the flyby of a star of mass $M_p = 0.8^{+0.1}_{-0.1} M_\odot$ passing on a parabolic orbit at $r_p = 110 \pm 10$ au and $i = 70^{+5}_{-10}$ explains several unaccounted-for outer solar system features. It quantitatively reproduces the orbital properties of the cold Kuiper belt population, Sedna-like objects and high-inclination TNOs. Unexpectedly, this flyby also accounts for the otherwise difficult-to-explain retrograde population. The model's beauty lies in its simplicity and ability to make specific predictions. These predictions include a distinct clustering in a , e , i space and a rise in the relative fraction of retrograde and Sedna-like TNOs. Future TNO discoveries may reveal the primordial solar system disk's size and structure.

Methods

Flyby simulations and selection procedure

Our parameter study consists of 3,080 individual simulations modelling the effect of stellar flybys on a planetesimal or debris disk surrounding the Sun. The aim was to find the subset of simulations that produces the various dynamics groups in the observed quantities and locations in the multidimensional parameter space. Previous work²⁴ found that the most promising parameter space for finding the most challenging TNO dynamical groups entails perturber masses in the range $M_p = 0.3$ – $1.0 M_\odot$, periastron distances $r_p = 50$ – 150 au, $i = 50^\circ$ – 70° and $\omega = 60^\circ$ – 120° . We scanned this parameter space in mass steps of $0.1 M_\odot$, r_p in steps of 10 au, i in units of 5° and ω with a variation of 10° .

The simulations start with an idealized thin disk³⁸ represented by $N = 10^4$ massless tracer particles. Taking the observed sizes of typically 100–500 au of protoplanetary and debris disks for guidance^{27,28}, we model disk sizes of 150 au and 300 au. We model the N gravitational three-body interactions between the Sun, the perturber star and each of the N test particles^{15,24,39}. Self-gravity and viscosity effects are negligible, as the interaction time is short ($< 30,000$ yr) and the disk's mass is considerably smaller than the Sun's ($m_d \ll 0.001 M_\odot$). We use a Runge–Kutta Cash–Karp scheme to determine the particle trajectories. The simulations start and end when the force of the perturber star on each particle is less than 0.1% (ref. 40). We optimize the computational effort by using an initial constant particle surface density to obtain a high resolution in the outer parts of the disk. We then post-process the

data by assigning different masses to the particles to model the actual mass density distribution^{41,42}.

We set strict standards for matching observations with simulations, rejecting 99.9% of all simulated cases. Nevertheless, this computational expense paid off. We obtained a near-perfect match to the known TNO population. We tested only for those TNOs not strongly coupled to Neptune ($T_N > 3.05$, where T_N is the Tisserand parameter). Thus, most resonant TNOs were excluded from the comparison. Similarly, we did not consider TNOs with $a > 10,000$ au, as more distant encounters and the galactic potential could affect their orbits over Gyr timescales. After the flyby, some objects enter into a resonant orbit with Neptune during our long-term simulation. They are not visible in Fig. 1 since they do not meet the $T_N > 3.05$ threshold. Probably the number of resonant objects is small because the simulation only covers the first 1 Gyr; additional resonant TNOs may be produced over extended periods. A higher resolution of the disk population would also be required to describe this process adequately. Moreover, resonant TNOs might be produced if Neptune migrated outward after the flyby.

We used a decision-tree-based inspection method, first selecting the flybys that avoid strong perturbations inside 30–35 au. We used the approximation $r_d = 0.28M_p^{-0.32}r_p$ (ref. 40) as an indicator of the radial distance r_d up to which the disk remains largely undisturbed. This equation applies only to coplanar encounters, while we study inclined encounters. Therefore, we slightly extend the parameter space to account for the difference. A subset of 490 simulations fulfilled the criterion of an unperturbed population up to 30–35 au. Here, we assume that the planets orbit at their current locations. If the solar system was in a more compact configuration during the flyby, the constraints would relax. Next, we retained only flybys that produce a cold Kuiper belt population and Sedna-like objects in suitable regions of the parameter space. Only a small subset clustering around perturber masses of 0.7–0.9 M_\odot and periastron distances of 90–110 au fulfils this criterion. Among the few remaining possibilities, additional cases can be excluded on more stringent criteria. For example, among the $r_p = 110$ cases, higher-mass perturbers ($M_p \geq 0.9 M_\odot$) tend to produce too few cold Kuiper belt objects, while lower-mass perturbers ($M_p \leq 0.7 M_\odot$) have difficulties reproducing the high-eccentricity TNOs. For 0.8 M_\odot perturbers, only perihelion distances of 100 au and 110 au can produce the right size of the unperturbed region. The closer encounter (100 au) produces 80% fewer cold TNOs than does the 110 au perturber. Hence, a 0.8 M_\odot perturber passing at a periastron distance of 110 au best fits the observational data.

We simultaneously tested for the inclinations and the argument of perihelion of the perturber's orbit. Again, the relative number of cold Kuiper belt objects is a key element. Supplementary Fig. 3 shows the dependence of the number of cold population particles on i and ω for a flyby with $M_p = 0.8 M_\odot$ at $r_p = 110$ au. The cold population decreases significantly below 70° inclination and 80° argument of perihelion. While above these values, the simulations do not reproduce the inclination and eccentricity distributions of the TNOs correctly. Hence, an inclination of 70° and an angle of perihelion of 80° produce the best fit.

We tested the best-fit flyby to check its influence on the giant planets' orbits. Our criterion is that the changes in i and e due to the flyby should be less than the difference of currently observed planetary orbits from being circular and in the plane. Neptune's orbit is more vulnerable than those of the other planets. However, the key parameter is the orbital position at the moment of flyby. Even Neptune's orbit remains nearly unaffected ($\Delta < \text{today's } e \text{ and } i$) at the locations indicated in blue in Supplementary Fig. 2. Uranus's eccentricity remains unaffected; however, small ranges of positions are excluded because the inclination is slightly higher (1°) than today's (0.7°). The influence on Jupiter and Saturn is negligible, independent of orbital location.

When performing such a comparison, we face two challenges: (i) the biases in the known TNO population^{1,2} and (ii) the fact that the size

of the primordial disk is unknown. Therefore, we determined three best fits emphasizing different populations (see Table 1). Model B gives a slightly larger cold population than does A1 (see Supplementary Fig. 4). Model C produces more high-inclination objects (see Supplementary Fig. 6). Models A1 and A2 only differ in their assumed disk sizes of 150 au and 300 au, respectively.

While this method was labour intensive, it was the most reliable approach. Automated statistical methods^{25,29} generally test against deviations from the median or mean. We find that taking a mean as the decision basis fails to account for multiple clustering in TNO dynamical groups, especially in multidimensional parameter space. Moreover, various observational biases make it problematic to compare 'unbiased' simulation results in an automated way. We also tested using the Outer Solar System Origins Survey observation simulator³², applying the default absolute magnitude distribution to assign magnitudes to the test particles. We find that, for model A1, 70 of our simulated objects should be currently observable. However, rating the quality of this match in an automated way faces the problem that the result depends sensitively on the size of the chosen comparison parameter space.

Long-term evolution

Determining the long-term evolution after the flyby requires a high-precision integrator, which makes these simulations computationally expensive. Therefore, we modelled the long term only for a subset of the results consisting of all particles fulfilling the conditions $35 \text{ au} < r_p < 90 \text{ au}$, $i < 60^\circ$ and $a < 2,000 \text{ au}$. These TNOs correspond to ~20% of the total TNO population and roughly to the TNOs that should be visible with instruments such as the Vera Rubin telescope. In addition to the test particles from the flyby simulation, the four outer giant planets were included in the long-term simulation. We start with the particle positions and velocities at 12,000 years after the perihelion passage. Using the GENGA code⁴³, we follow the trajectories of the test particles for the next 1 Gyr. These trajectories are determined using a hybrid symplectic integrator.

Flyby frequency determination

We determined the occurrence rate of such close flybys in different cluster environments ranging from short-lived low- N clusters to massive, compact, long-lived clusters. We performed an extensive set of N -body simulations using the code Nbody 6++ (ref. 44). In these simulations (for details see ref. 36), the cluster development matches that of observed clusters regarding the temporal development of the cluster mass and size with cluster age. We computed hundreds of realizations so that the results have high statistical relevance. We record the parameters of any close interaction between two stars and use this information in a post-processing step to determine the effect of each encounter on the disk size (equal to the unperturbed area after an encounter). We study the subset of solar-type stars and test for the frequency of encounters leading to a 30–50 au-sized unperturbed disk. We also test for solar-type stars encountering a perturber of mass 0.6–1.0 M_\odot at a distance of 90–130 au, similar to our best-fit results.

Toy model for effect on the Oort cloud

We estimated the effect of such a flyby on a potentially existing Oort cloud. Our toy model consisted of 10,000 particles randomly distributed in a 100,000 au-sized sphere surrounding the Sun. We simulated model A's flyby effect on this Oort cloud. The particle trajectories are calculated using the REBOUND N -body code⁴⁵ employing IAS15, a 15th-order Gauss–Radau integrator⁴⁶.

Data availability

The data of the complete parameter study are available on the DESTINY database at <https://destiny.fz-juelich.de>. Source data are provided with this paper.

Code availability

REBOUND and GENGA are open access codes. The DESTINY code will be available upon reasonable request. However, the DESTINY database (<https://destiny.fz-juelich.de>) also allows diagnostics to be performed online. It allows to reproduce Fig. 2, and also similar plots for the entire parameter study. A complete illustration of the dynamics of the flyby scenario of model A1 is available in Supplementary Video 1.

References

- Gladman, B. & Volk, K. Transneptunian space. *Annu. Rev. Astron. Astrophys.* **59**, 203–246 (2021).
- Kavelaars, J. J., Lawler, S. M., Bannister, M. T. & Shankman, C. in *The Trans-Neptunian Solar System* (eds Prialnik, D. et al.) 61–77 (Elsevier, 2020).
- Fernandez, J. A. & Ip, W.-H. Some dynamical aspects of the accretion of Uranus and Neptune: the exchange of orbital angular momentum with planetesimals. *Icarus* **58**, 109–120 (1984).
- Hahn, J. M. & Malhotra, R. Orbital evolution of planets embedded in a planetesimal disk. *Astron. J.* **117**, 3041–3053 (1999).
- Gomes, R. S. The origin of the Kuiper belt high-inclination population. *Icarus* **161**, 404–418 (2003).
- Morbidelli, A., Brown, M. E. & Levison, H. F. The Kuiper belt and its primordial sculpting. *Earth Moon Planets* **92**, 1–27 (2003).
- Levison, H. F., Morbidelli, A., Van Laerhoven, C., Gomes, R. & Tsiganis, K. Origin of the structure of the Kuiper belt during a dynamical instability in the orbits of Uranus and Neptune. *Icarus* **196**, 258–273 (2008).
- Raymond, S. N., Izidoro, A. & Morbidelli, A. in *Planetary Astrobiology* (eds Meadows, V. S. et al.) 287–324 (Univ. of Arizona, 2020).
- Brown, M. E., Trujillo, C. & Rabinowitz, D. Discovery of a candidate inner Oort cloud planetoid. *Astrophys. J.* **617**, 645–649 (2004).
- Trujillo, C. A. & Sheppard, S. S. A Sedna-like body with a perihelion of 80 astronomical units. *Nature* **507**, 471–474 (2014).
- Sheppard, S. S., Trujillo, C. A., Tholen, D. J. & Kaib, N. A new high perihelion trans-Plutonian inner Oort cloud object: 2015 TG387. *Astron. J.* **157**, 139 (2019).
- Gladman, B. et al. Discovery of the first retrograde transneptunian object. *Astrophys. J. Lett.* **697**, 91–94 (2009).
- Chen, Y.-T. et al. Discovery of a new retrograde trans-Neptunian object: hint of a common orbital plane for low semimajor axis, high-inclination TNOs and centaurs. *Astrophys. J. Lett.* **827**, 24 (2016).
- Punzo, D., Capuzzo-Dolcetta, R. & Portegies Zwart, S. The secular evolution of the Kuiper belt after a close stellar encounter. *Mon. Not. R. Astron. Soc.* **444**, 2808–2819 (2014).
- Kobayashi, H. & Ida, S. The effects of a stellar encounter on a planetesimal disk. *Icarus* **153**, 416–429 (2001).
- Kenyon, S. J. & Bromley, B. C. Stellar encounters as the origin of distant Solar System objects in highly eccentric orbits. *Nature* **432**, 598–602 (2004).
- Kobayashi, H., Ida, S. & Tanaka, H. The evidence of an early stellar encounter in Edgeworth Kuiper belt. *Icarus* **177**, 246–255 (2005).
- Dai, F., Facchini, S., Clarke, C. J. & Haworth, T. J. A tidal encounter caught in the act: modelling a star-disc fly-by in the young RW Aurigae system. *Mon. Not. R. Astron. Soc.* **449**, 1996–2009 (2015).
- Rodríguez, J. E. et al. Multiple stellar flybys sculpting the circumstellar architecture in RW Aurigae. *Astrophys. J.* **859**, 150 (2018).
- De Rosa, R. J. & Kalas, P. A near-coplanar stellar flyby of the planet host star HD 106906. *Astron. J.* **157**, 125 (2019).
- Winter, A. J., Booth, R. A. & Clarke, C. J. Evidence of a past disc-disc encounter: HV and DO Tau. *Mon. Not. R. Astron. Soc.* **479**, 5522–5531 (2018).
- Akiyama, E. et al. A tail structure associated with a protoplanetary disk around SU Aurigae. *Astron. J.* **157**, 165 (2019).
- Ménard, F. et al. Ongoing flyby in the young multiple system UX Tauri. *Astron. Astrophys.* **639**, L1 (2020).
- Pfalzner, S., Bhandare, A., Vincke, K. & Lacerda, P. Outer Solar System possibly shaped by a stellar fly-by. *Astrophys. J.* **863**, 45 (2018).
- Moore, N. W. H., Li, G. & Adams, F. C. Inclination excitation of Solar System debris disk due to stellar flybys. *Astrophys. J.* **901**, 92 (2020).
- LSST Science Collaborations LSST Science Book, Version 2.0. Preprint at <https://doi.org/10.48550/arXiv.0912.0201> (2009).
- Andrews, S. M. Observations of protoplanetary disk structures. *Annu. Rev. Astron. Astrophys.* **58**, 483–528 (2020).
- Hendler, N. et al. The evolution of dust disk sizes from a homogeneous analysis of 1–10 Myr old stars. *Astrophys. J.* **895**, 126 (2020).
- Jílková, L., Portegies Zwart, S., Pijloo, T. & Hammer, M. How Sedna and family were captured in a close encounter with a solar sibling. *Mon. Not. R. Astron. Soc.* **453**, 3157–3162 (2015).
- Batygin, K. & Brown, M. E. Generation of highly inclined trans-Neptunian objects by Planet Nine. *Astrophys. J. Lett.* **833**, 3 (2016).
- Batygin, K., Morbidelli, A., Brown, M. E. & Nesvorný, D. Generation of low-inclination, Neptune-crossing trans-Neptunian objects by Planet Nine. *Astrophys. J. Lett.* **966**, 8 (2024).
- Bannister, M. T. et al. OSSOS. VII. 800+ trans-Neptunian objects—the complete data release. *Astrophys. J. Suppl.* **236**, 18 (2018).
- Bernardinelli, P. H. et al. A search of the full six years of the Dark Energy Survey for outer Solar System objects. *Astrophys. J. Suppl.* **258**, 41 (2022).
- Sheppard, S. S., Trujillo, C. & Tholen, D. J. Beyond the Kuiper belt edge: new high perihelion trans-Neptunian objects with moderate semimajor axes and eccentricities. *Astrophys. J. Suppl.* **825**, 13 (2016).
- Nesvorný, D., Bernardinelli, P., Vokrouhlický, D. & Batygin, K. Radial distribution of distant trans-Neptunian objects points to Sun's formation in a stellar cluster. *Icarus* **406**, 115738 (2023).
- Pfalzner, S. & Vincke, K. Cradle(s) of the Sun. *Astrophys. J.* **897**, 60 (2020).
- Portegies Zwart, S. Oort cloud Ecology. I. Extra-solar Oort clouds and the origin of asteroidal interlopers. *Astron. Astrophys.* **647**, 136 (2021).
- Pringle, J. E. Accretion discs in astrophysics. *Annu. Rev. Astron. Astrophys.* **19**, 137–162 (1981).
- Musiela, Z. E. & Quarles, B. The three-body problem. *Rep. Prog. Phys.* **77**, 065901 (2014).
- Breslau, A., Steinhausen, M., Vincke, K. & Pfalzner, S. Sizes of protoplanetary discs after star-disc encounters. *Astron. Astrophys.* **565**, 130 (2014).
- Hall, S. M., Clarke, C. J. & Pringle, J. E. Energetics of star-disc encounters in the non-linear regime. *Mon. Not. R. Astron. Soc.* **278**, 303–320 (1996).
- Steinhausen, M., Olczak, C. & Pfalzner, S. Disc-mass distribution in star-disc encounters. *Astrophys. J.* **538**, 10 (2012).
- Grimm, S. L. & Stadel, J. G. The GENGA code: gravitational encounters in *N*-body simulations with GPU acceleration. *Astrophys. J.* **796**, 23–39 (2014).
- Aarseth, S. J. *Gravitational N-Body Simulations* (Cambridge Univ. Press, 2003).
- Rein, H. & Liu, S.-F. REBOUND: an open-source multi-purpose *N*-body code for collisional dynamics. *Astron. Astrophys.* **537**, 128 (2012).
- Rein, H. & Spiegel, D. S. IAS15: a fast, adaptive, high-order integrator for gravitational dynamics, accurate to machine precision over a billion orbits. *Mon. Not. Astron. Soc.* **446**, 1424–1437 (2015).

Acknowledgements

We thank S. Habbinga for her assistance in the visualization of model A1, M. Bannister and R. Dorsey for advising us on interpreting TNO survey results and the Outer Solar System Origins Survey simulator and F. Wagner for supporting us in implementing the code GENGA on the FZJ system. S.P. has received funding for this project through grant 450107816 of the Deutsche Forschungsgemeinschaft.

Author contributions

Conceptualization, S.P.; simulation of the parameter study, long-term evolution and effect of Oort cloud, A.G.; diagnostic, S.P., A.G.; comparison with observational data, A.G., S.P., S.P.Z.; writing, S.P., A.G., S.P.Z.; funding acquisition and resources, S.P.; supervision, S.P.; data curation, A.G.

Funding

Open access funding provided by Forschungszentrum Jülich GmbH.

Competing interests

The authors declare no competing interests.

Additional information

Supplementary information The online version contains supplementary material available at <https://doi.org/10.1038/s41550-024-02349-x>.

Correspondence and requests for materials should be addressed to Susanne Pfalzner.

Peer review information *Nature Astronomy* thanks Pedro Bernardinelli and the other, anonymous, reviewer(s) for their contribution to the peer review of this work.

Reprints and permissions information is available at www.nature.com/reprints.

Publisher's note Springer Nature remains neutral with regard to jurisdictional claims in published maps and institutional affiliations.

Open Access This article is licensed under a Creative Commons Attribution 4.0 International License, which permits use, sharing, adaptation, distribution and reproduction in any medium or format, as long as you give appropriate credit to the original author(s) and the source, provide a link to the Creative Commons licence, and indicate if changes were made. The images or other third party material in this article are included in the article's Creative Commons licence, unless indicated otherwise in a credit line to the material. If material is not included in the article's Creative Commons licence and your intended use is not permitted by statutory regulation or exceeds the permitted use, you will need to obtain permission directly from the copyright holder. To view a copy of this licence, visit <http://creativecommons.org/licenses/by/4.0/>.

© The Author(s) 2024